J Musculoskelet Neuronal Interact 2006; 6(3):251-257

Original Article

Hylonome

Subchondral bone failure in overload arthrosis: A scanning electron microscopic study in horses

R.W. Norrdin[1] and S.M. Stover[2]

[1]Department of Microbiology Immunology and Pathology, College of Veterinary Medicine and Biomedical Sciences, Colorado State University, Fort Collins CO, USA; [2]J.D. Wheat Veterinary Orthopedic Research Laboratory, School of Veterinary Medicine, University of California at Davis, Davis CA, USA

Abstract

Mechanical overload leads to a common arthrosis in the metacarpal condyle of the fetlock joint of racehorses. This is usually asymptomatic but severe forms can cause lameness. Subchondral bone failure is often present and the predictability of the site provided an opportunity to study of the progression of bone failure from microcracks to actual collapse of subchondral bone. Twenty-five fetlock condyles from racehorses with various stages of disease were selected. Stages ranged from mild through severe subchondral bone sclerosis, to the collapse of bone and indentation or loss of cartilage known as 'traumatic osteochondrosis'. Parasagittal slices were radiographed and examined with scanning electron microscopy. Fine matrix cracks were seen in the subchondral bone layer above the calcified cartilage and suggested loss of water or other non-collagenous components. The earliest microcracks appeared to develop in the sclerotic bone within 1-3 mm of the calcified cartilage layer and extend parallel to it in irregular branching lines. Longer cracks or microfractures appeared to develop gaps as fragmentation occurred along the margins. Occasional osteoclastic resorption sites along the fracture lines indicated activated remodeling may have caused previous weakening. In one sample, smoothly ground fragments were found in a fracture gap. Bone collapse occurred when there was compaction of the fragmented matrix along the microfracture. Bone collapse and fracture lines through the calcified cartilage were associated with indentation of articular cartilage at the site.

Keywords: Equine, Arthrosis, Subchondral Bone, Microfracture, Scanning Electron Microscopy

Introduction

Sclerotic thickening of subchondral bone is important in the pathogenesis of arthrosis[1,2] and changes in the subchondral bone plate may be more important than those in the underlying trabeculae[3,4]. Excessive loading and the accumulation of microdamage are thought to be important factors[5]. Changes in the type[6] but not necessarily the quantity of microdamage[7] have been found in osteoarthritis. The mechanisms by which this leads to bone failure is unclear. It may involve altered cytokine expression[8] and apoptosis of osteocytes[9] associated with stimulation of remodeling. Devitalized bone is resistant to remodeling and this is thought to allow the accumulation of microdamage[5,10]. Vascular disturbances that cause subchondral bone necrosis may also be involved[11,12]. The mechanisms probably vary with the specific joint depending on the forces involved and the pattern of loading[2]. Although there have been studies on the quantitation of microdamage in arthritic joints, there is little information on the progression of bone failure from microcracks to actual collapse of subchondral bone.

Subchondral sclerosis and areas of bone devitalization are common in the overload arthrosis of equine athletes[13,14]. Actual subchondral bone failure occurs focally in the palmar metacarpal condyle of the fetlock joint (Figure 1) where indentation and collapse of the articular cartilage is seen. This is referred to as 'traumatic osteochondrosis'[14,15]. It is primarily a disease of racehorses and is very common in the US. It is often asymptomatic but more severe forms are asso-

The authors have no conflict of interest.

Corresponding author: Robert W. Norrdin, DVM, Ph.D., College of Veterinary Medicine and Biomedical Sciences, Colorado State University, Fort Collins CO, 80523, USA
E-mail: rnorrdin@colostate.edu

Accepted 30 March 2006

Figure 1. Equine fetlock joint. The area on the palmar surface of the condyle where overload arthrosis and subchondral bone failure occurs is indicated with arrows.

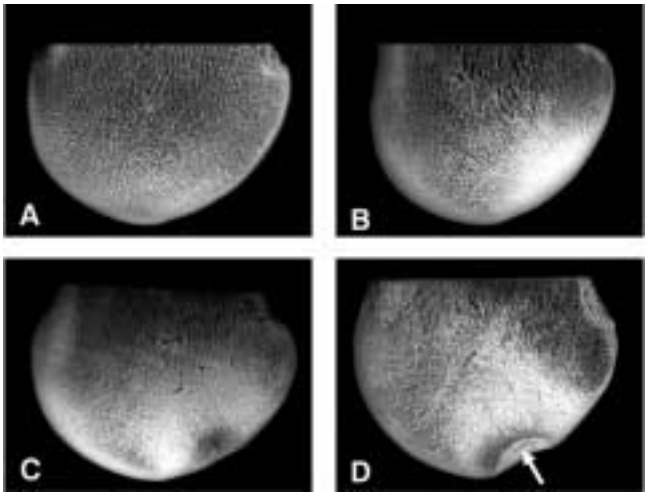

Figure 2. Radiographs of 4 mm condylar slices used for SEM. These show the spectrum of changes studied. **A**: Minimal/mild sclerosis. **B**: Severe sclerosis. **C**: Severe sclerosis with focal radiolucency/rarefaction. **D**: Advanced lesion with subchondral bone failure consisting of collapse with microfracture in more dense bone (arrow) and indentation of cartilage.

ciated with fetlock lameness[13]. The consistency of the site makes it a useful model in which to study the bone changes leading to failure. The objective of this work was to study morphologic changes at the site in condyles with various stages of disease using scanning electron microscopy (SEM).

Materials and methods

Twenty-five fetlock condyles collected at necropsy from 23 thoroughbred racehorses that were racing, training or involved in accidents at the time of death or euthanasia were used in the study. Twenty of the samples were from condyles selected on the basis of radiographs for having mild, moderate or severe subchondral sclerosis, and severe sclerosis with focal radiographic rarefaction. In these samples, cartilage collapse and osteochondrosis had not yet occurred at the lesion site on the palmar condyle. There were five samples in each group. These had been used to study strain patterns at the site of failure[16]. An additional five condyles from three horses with cartilage flattening, infolding or loss, indicating more advanced lesion with subchondral bone failure typical of 'osteochondrosis', were also studied.

A 4 mm parasagittal slice was cut through the lesion site at midcondyle or just lateral to midcondyle where slices had been taken for strain studies. Contact radiographs were made of the slices to confirm the severity of sclerosis and pattern of rarefaction, and look for gross microfractures and bone collapse. Slices were digested in 7.5% bleach solution for 24 hours to remove soft tissue. The palmar half of the condyles were rinsed in water and ground with wettable sandpaper followed by polishing with a cloth and powder. Specimens were then sonicated, defatted in acetone for 24 hours and dried. Mounted specimens were sputter-coated with gold and examined on a Phillips XL30 scanning electron microscope.

The entire sample was scanned at 30x for microcracks, microfractures and other changes indicative of matrix failure. These were referred to as failure lesions. The palmar injury site was identified at two thirds to three-fourths the distance from the proximal articular margin to the apex of the condyle. Representative fields were recorded at 30x, 100x and 800x. Additional images were collected of areas with changes at the site. At 30x, the fields were approximately 3.5 mm in height and included the area in which cracks and microfractures usually developed. The three adjacent fields above the cartilage surface were also recorded at 30x, 100x and (usually) 800x. This allowed identification of failure lesions and comparison of matrix and lacunae in the sclerotic lesion site and the overlying sclerotic and trabecular bone at a level as great as 14 mm. Microcracks were recognized as discrete linear cracks that were generally longer than matrix cracks and extended across one or more osteons. There was little or no separation but some irregularities might be seen along the margins. Often, multiple microcracks were seen in a pattern that suggested stress effects. Microfractures were longer linear defects in which a gap had developed and fragmentation along the gap margin could be seen. Larger microfractures could be seen radiographically.

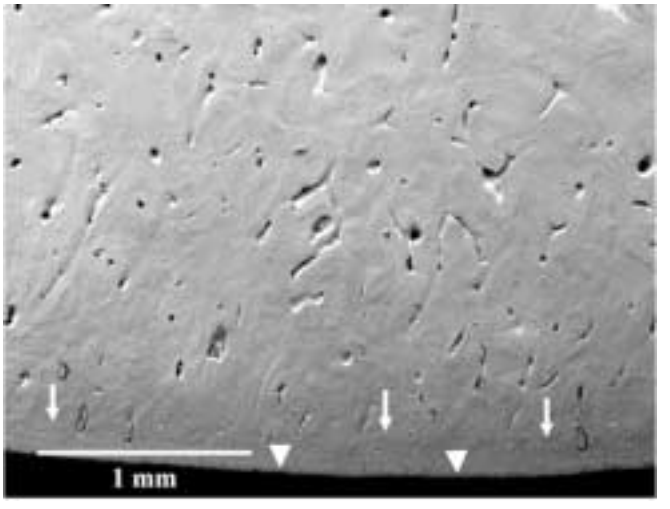

Figure 3. Unaffected palmar subchondral bone site from a sample in the group with mild sclerosis. Non-calcified articular cartilage is present at the bottom (arrowheads). The interface of the calcified cartilage and bone can be seen in places (arrows).

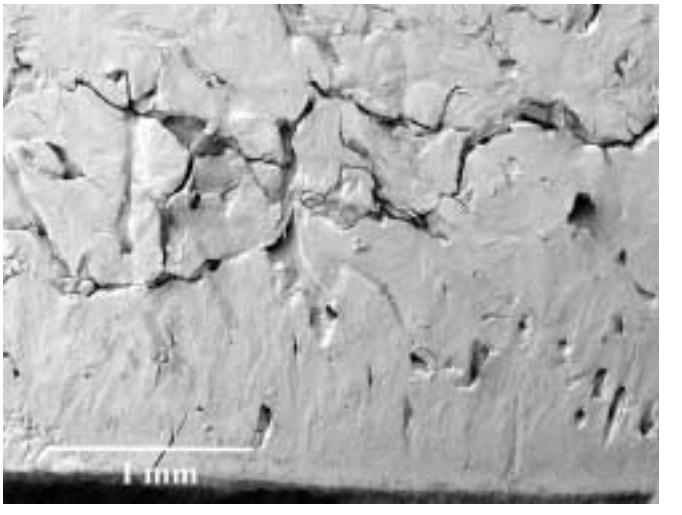

Figure 4. Subchondral bone with microfracture lines and early collapse in a sample from the group with severe sclerosis and focal rarefaction. Note multiple cracks and fragmentation of bone with formation of gaps within fracture lines.

Results

Radiographs

Radiographs confirmed that a spectrum of changes was present in the samples examined (Figure 2). These ranged from increasing severity of sclerosis to focal rarefaction in the sclerotic zone and collapse of subchondral bone with cartilage flattening or infolding. In one of the more severely affected samples there was a radiolucent microfracture parallel to the articular surface in more dense bone (Figure 2).

Matrix and osteocyte lacunae

Matrix changes were difficult to distinguish from possible processing artifact but some observations were made. The palmar site often had increased prominence of the lamellar pattern in the bone just above the calcified cartilage layer in the sclerotic zone. Milder change was seen at the same level of the subchondral bone away from the lesion site. This change was seen in all groups but considered to be more easily distinguishable with increasing severity of sclerosis. It was not seen in the trabecular bone at higher levels. The change was attributable to a more coarse appearance of the matrix with fine transverse cracks separating collagen fibers within the lamellae making the osteonal pattern more prominent. Fine, spider-like cracks could also be found in the adjacent matrix. This pattern suggested fine cracks developed from drying and shrinkage, i.e., loss of water and/or other components of the non-collagenous matrix. These fine cracks sometimes involved the margins of osteocyte lacunae but did not appear to be centered here. Generally, osteocyte lacunae and canaliculi varied somewhat in appearance but no consistent changes were appreciated in comparing lacunae in subchondral bone from samples with varying severity of sclerosis and lesions. Nor were changes seen in comparing lacunae in the subchondral bone to those in the overlying trabeculae.

Microcracks and microfractures

No failure lesions were seen in the groups with mild, moderate or severe sclerosis (Figure 3). Lesions consisting of sub-gross cracks, i.e., microcracks or microfractures were seen in three of the five samples in the group with severe sclerosis and rarefaction, but a distinct fracture gap was present in only one of these. Sub-gross cracks were seen in all five of the samples from the group of condyles with more advanced lesions in which cartilage flattening, infolding, or erosion had occurred. A microfracture with a distinct gap was visible in four of the five.

The smallest and presumably earliest microcracks in the subchondral bone were within 1-3 mm of the calcified cartilage layer. Developing cracks extended parallel to the surface in irregular lines with minor branching. As the crack enlarged to become a microfracture, fragmentation of the edges at the sites of irregularity and development of gaps was seen (Figure 4). The mismatched edges of the microfracture indicated where there had been loss as well as fragmentation of bone as a gap developed. In some failure lesions, evidence of osteoclastic erosion was found (Figure 5) indicating there had been activation of remodeling at the site. Generally, however, the smaller, earlier cracks and microfractures found in the dense, sclerotic bone just above the calcified cartilage layer had no evidence of osteoclastic resorption.

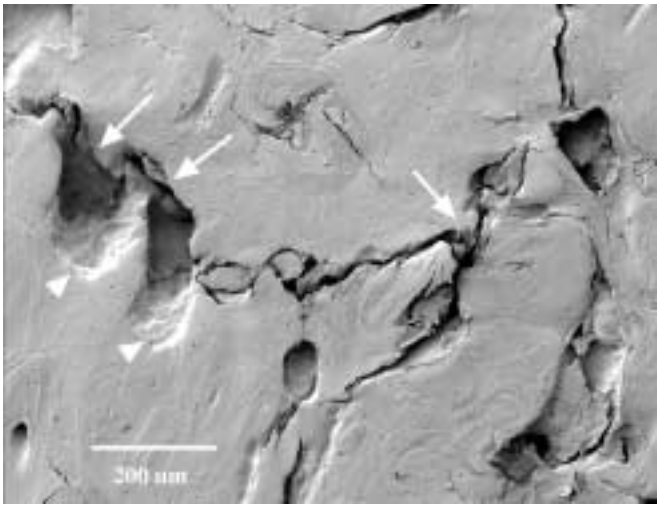

Figure 5. Higher magnification of area along the developing microfracture in Figure 4. Note mismatched surfaces (arrows) and fragmentation of margins indicating fracture gap has collapsed. Osteoclastic erosion sites (arrowheads) were seen in larger developing cracks and indicated there had been remodeling at the site.

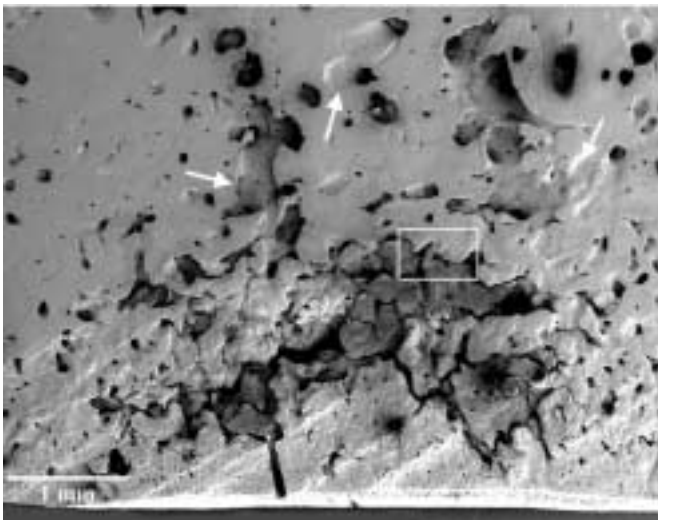

Figure 6. Incompletely ground sample from group with advanced lesions shows gap in defect containing smoothly ground fragments of subchondral bone. (Region of interest in block is magnified in Figure 7). Enlarged vascular canals and resorption sites (arrows) indicate there has been activated remodeling around the more chronic defect.

In one incompletely ground sample, a cavity could be visualized in the fracture gap in which bone fragments as well as an entrapped vessel were present (Figure 6). The fragments had rounded, smooth surfaces that appeared to be the result of a chronic grinding action. The margins of the gap were rounded and smooth as well (Figure 7). They were surrounded by enlarged vascular channels and osteoclast resorption sites. This sample was from a horse that was killed because of catastrophic injury to the contralateral front leg. This indicated that the animal had been active in racing or training and there was little disability associated with the failure lesion.

The overlying cartilage was generally intact. Enfolding of the cartilage occurred when there was loss of the subchondral bone, apparently as a result of mechanical grinding or compaction of fragments in the gap of a more extensive microfracture. At one indented site, a perpendicular fracture through the calcified cartilage layer was connected to the microfracture and associated with further infolding (Figure 8). There were multiple fragmentation lines and a compacted appearance in the overlying layer of bone (Figures 8,9). There was little or no evidence of woven bone or other reactive change at the failure site. However, evidence of osteoclastic enlargement of vascular canals was often seen in the bone above the failure lesion site (Figure 10). These could be recognized radiographically as a halo of radiating channels around the failure site (Figure 2).

Figure 7. Higher magnification of microfracture gap with entrapped vessel from Figure 6. Note smooth edges on ground fragments indicating chronic wear on the surfaces.

Discussion

In this SEM study of subchondral bone failure, a spectrum of changes was seen that suggested the sequence of changes in the development of microfractures and collapse of bone. The shortest and presumably earliest microcracks were seen in the sclerotic bone within 1-3 mm of the cartilage cover. This was in the center of the area in which there was a progressive increase in the radiographic density of trabeculae and subchondral bone plate. There is often a zone of pallor in the bone at this site and debris-plugged marrow vascular channels and devitalized bone can be seen histologically[14].

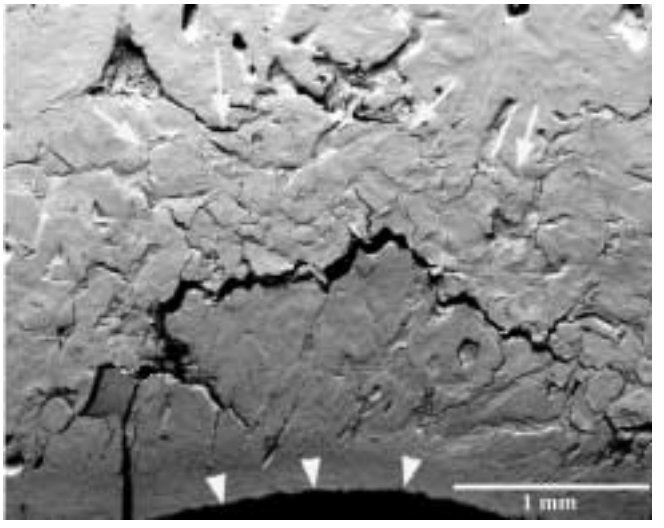

Figure 8. Subchondral bone microfracture at the site of collapse and indentation of cartilage (arrowheads) in a sample from the group with advanced lesions. A fracture line through the calcified cartilage (lower left) is associated with further infolding.The layer of bone above the microfracture has multiple fragmentation lines and a compacted appearance (outlined by arrows).

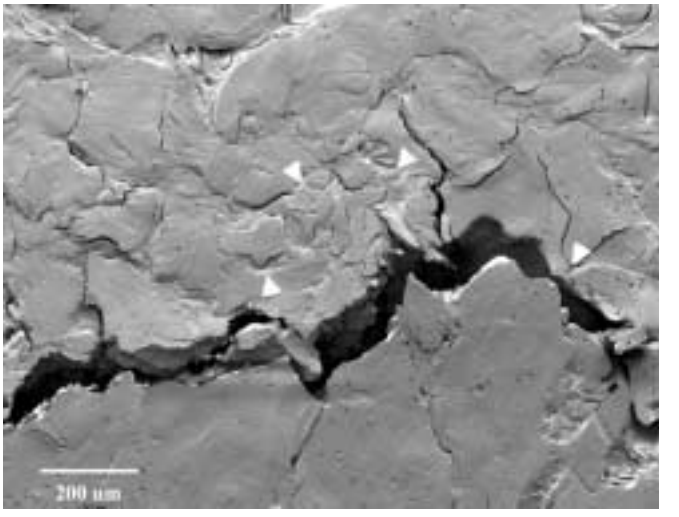

Figure 9. Higher magnification of subchondral bone microfracture with collapsed matrix from Figure 7. Bone matrix above the microfracture line has multiple fine cracks (arrowheads) and a compacted arrangement. Also note continued fragmentation of fracture margins in the gap.

Ischemia and poor perfusion through the sclerotic matrix has been proposed as the cause of this devitalization[14,15]. Although devitalized bone can be recognized histologically by loss of osteocytes, no consistent changes in osteocyte lacunae could be appreciated in the ground sections used for scanning microscopy. Matrix change may make the site susceptible to microcracking. The only matrix variation seen in this SEM study was the fine cracks seen within the lamellae and interstitial matrix that were found in the zone above the calcified cartilage and considered more distinguishable in the samples with increasing sclerosis. This change suggested a drying artifact that made the osteonal collagen/lamellar patterns of the bone more prominent. Because drying was involved in the preparation of these samples and no controls were available, this was most likely an artifact of processing. The greater prominence of the change in the bone above the calcified cartilage may reflect increased grinding and polishing required in the sclerotic bone. It is a possibility, however, that the change itself, or the artifact of processing, is attributable to the loss of water and/or other non-collagenous matrix components at this site *in vivo*. This would be compatible with decreased perfusion through thickened bone that contains dead osteocytes and plugged canaliculi. Additional studies are needed to clarify this point.

Mechanical forces are no doubt responsible for the development of microcracks at this site. It has been shown that exercise in young horses leads to increased diffuse basic fuchsin staining indicative of microdamage at the palmar site[14] and there is evidence of stimulated remodeling at the cartilage bone interface where sclerosis develops[17]. More dense bone is seen clinically[18]. The forces at the site are probably complex. When *ex vivo* slices of sclerotic condyles were subjected to direct compression perpendicular to the articular surface, there was a transfer of strains through the sclerotic zone to the overlying trabeculae. No consistent change was seen at the lesion site[16]. More complex force patterns must be involved

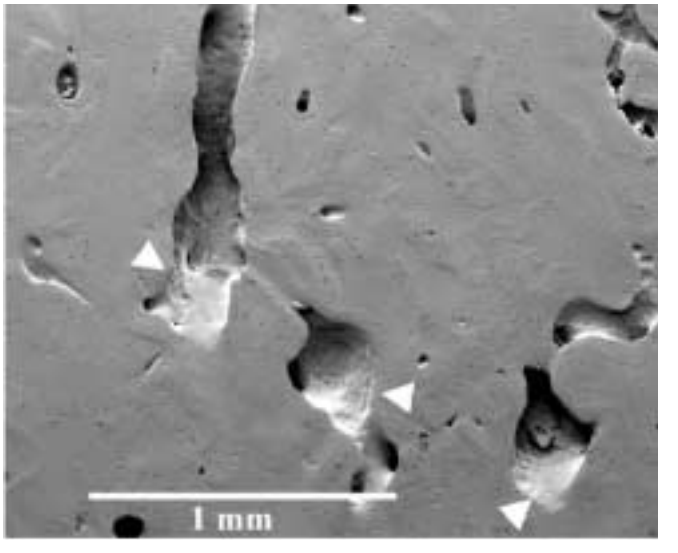

Figure 10. Larger vascular canals with osteoclastic resorption sites (arrowheads) were often seen at higher levels in the subchondral bone (from sample in the group with advanced lesions). The enlarged vascular canals were recognizable radiographically.

during joint motion that focus forces on this site.

The smallest microcracks appeared to perpetuate across osteonal boundaries to become larger microfractures. These developed gaps as fragmentation occurred along their margins. In some of these, evidence of osteoclastic resorption was seen. This implies that there was access to this area by viable adjacent tissue bearing such cells. Mismatched fracture margins at the sites of erosion indicate that erosion weakened the matrix. Riggs et al.[19] have studied this condylar lesion and found sites of resorption at an interface between hypermineralized bone and bone of normal mineral density about 2 mm above the calcified cartilage. They suggest this was induced by microdamage from excessive shear at the interface and weakens the site. This is compatible with the occurrence of Howships lacunae in the microfractures seen in the present study. The original site of failure may vary. Perhaps smaller microcracks originate in the sclerotic zone and gaps develop when they extend to areas of resorption that has weakened the bone. Alternatively, the resorption may be a remodeling response to the microdamage itself and the resulting bone loss has contributed to the progression of these more long-standing lesions.

In the sample in which total collapse had not occurred, the cavity of fragments with rounded edges indicated movement and grinding had occurred over a period of time. The fact that this sample came from a horse still racing suggests that there was no significant lameness associated with such a lesion or that there was anesthesia at the site that allowed continued abuse mechanically. Along with the lack of reactive change such as woven bone formation, these changes are compatible with devitalized bone. In *ex vivo* compressive loading of a condyle in which a crack had developed at the site, it closed and opened freely on loading and unloading with off-scale shear strains[16]. This opening and closing action is presumably responsible for the grinding of fragments in the gap. The development of a gap with fragmented matrix probably corresponds to the stage at which focal radiolucency develops in the sclerotic zone. The osteoclastic erosion seen in vascular channels above the sclerotic zone corresponds to the enlargement of radially arranged vessels seen radiographically. Such erosion increases porosity within the sclerotic subchondral bone which is usually approximately 80% bone[14]. This allows for the compaction of the matrix as collapse of bone occurs. The collapse of matrix appears to occur primarily above the microfracture where multiple microcracks and fragmentation lines could be found in the compacted matrix. The compacted bone may account for the increased radiodensity sometimes seen beneath the indented surface at the lesion site. Additional cracks through the calcified layer were associated with the infolding of cartilage. These may have been contributory to the infolding or resulted from it. The indentation and infolding of cartilage lead to the later fragmentation and loss typical of 'traumatic osteochondrosis'.

In summary, this SEM study of subchondral bone failure in overload arthrosis suggests that small cracks develop into larger fractures as cracks branch and fragmentation occurs at the crack margins. The process is accompanied by activation of remodeling and osteoclastic resorption may contribute to weakening of the site. Collapse of bone is attributable to compaction of fragmented bone along the fracture margins. This allows flattening, indentation and enfolding of the superficial cartilage at the site.

Acknowledgements

This study was funded by grant DOO EQ-23 from the Morris Animal Foundation. The authors gratefully acknowledge the collection of specimens by Dr. Derek Read and colleagues, California State Veterinary Diagnostic Laboratory at San Bernardino, CA, and colleagues at the Colorado State University Veterinary Diagnostic Laboratory, Fort Collins, CO.

References

1. Radin EL, Ehrlich MG, Chernack R, Abernathy P, Paul P, Rose RM. Effect of repetitive impulsive loading on the knee joints of rabbits. Clin Orthop 1978; 131:288-293.
2. Kawcak CE, McIlwraith CW, Norrdin RW, Park RD, James SP. The role of subchondral bone in joint disease: a review. Equine Vet J 2001; 33:120-126.
3. Burr DB, Radin EL. Microfractures and microcracks in subchondral bone: are they relevant to osteoarthrosis? Rheum Dis Clin North Am 2003; 29:675-685.
4. Burr DB. Anatomy and physiology of the mineralized tissues: role in the pathogenesis of osteoarthrosis. Osteoarthritis Cartilage 2004; 12(Suppl.A):S20-30.
5. Frost HM. Perspectives: a biomechanical model of the pathogenesis of arthroses. Anat Rec 1994; 240:19-31.
6. Fazzalari NL, Kuliwaba JS, Forwood MR. Cancellous bone microdamage in the proximal femur: influence of age and osteoarthritis on damage morphology and regional distribution. Bone 2001; 31:697-702.
7. Mori S, Harruff R, Ambrosius W, Burr DB. Trabecular bone volume and microdamage accumulation in the femoral heads of women with and without femoral neck fractures. Bone 1997; 21:521-526.
8. Fazzalari NL, Kuliwaba JS, Findlay DM, Forwood MR. Microdamage distribution and altered messenger RNA gene expression in the proximal femur. Bone 2001; 28(Suppl.):S105.
9. Verborgt O, Gibson GJ, Schaffler MB. Loss of osteocyte integrity in association with microdamage and bone remodeling after fatigue *in vivo*. J Bone Miner Res 2000; 15:60-67.
10. Dunstan CR, Somers NM, Evans RA. Osteocyte death and hip fracture. Calcif Tissue Int 1993; 53(Suppl.1): S113-116.
11. Imhof H, Breitenseher M, Kainberger F, Trattnig S. Degenerative joint disease: cartilage or vascular disease? Skeletal Radiol 1997; 26:398-403.
12. Wong SY, Evans RA, Needs C, Dunstan CR, Hills E, Garvan J. The pathogenesis of osteoarthritis of the hip.

Evidence for primary osteocyte death. Clin Orthop 1987; 214:305-312.
13. Hornoff WJ, O'Brien TR, Pool RR. Osteochondritis dissecans of the distal metacarpus in the adult racing thoroughbred horse. Vet Radiol 1981; 22:98-106.
14. Norrdin RW, Kawcak CE, Capwell BA, McIlwraith CW. Subchondral bone failure in an equine model of overload arthrosis. Bone 1998; 22:133-139.
15. Pool RR, Meagher DM. Pathologic findings and pathogenesis of racetrack injuries. Vet Clin North Am Equine Pract 1990; 6:1-30.
16. Norrdin RW, Bay BK, Drews MJ, Martin RB, Stover SM. Overload arthrosis: strain patterns in the Equine metacarpal condyle. J Musculoskelet Neuronal Interact 2001; 1:357-362.
17. Norrdin RW, Kawcak CE, Capwell BA, McIlwraith CW. Calcified cartilage morphometry and its relation to subchondral bone remodeling in equine arthrosis. Bone 1999; 24:109-114.
18. Kawcak CE, McIlwraith CW, Norrdin RW, Park RD, Steyn PS. Clinical effects of exercise on subchondral bone of carpal and metacarpophalangeal joints in horses. Am J Vet Res 2000; 61:1252-1258.
19. Riggs CM, Whitehouse GH, Boyde A. Pathology of the distal condyles of the third metacarpal and metatarsal bones of the horse. Equine Vet J 1999; 31:140-148.